Electronic Supplementary Information

Reversible redox-responsive $^{1}H/^{19}F$ MRI molecular probes

Hongming Chen,[‡,a] Xiaoxue Tang,[‡,a] Xuanqing Gong,[a] Dongxia Chen,[a] Ao Li,[a] Chengjie Sun,[a] Hongyu Lin*[,a], and Jinhao Gao*[,a,b]

[a]State Key Laboratory of Physical Chemistry of Solid Surfaces, The MOE Laboratory of Spectrochemical Analysis & Instrumentation, The Key Laboratory for Chemical Biology of Fujian Province, and Department of Chemical Biology, College of Chemistry and Chemical Engineering, Xiamen University, Xiamen 361005, China.

[b]Center for Molecular Imaging and Translational Medicine, School of Public Health, Xiamen University, Xiamen 361005, China.

[‡]These authors contributed equally to this work.

*E-mail: hylin007@xmu.edu.cn; jhgao@xmu.edu.cn

Experimental sections

Materials and instrumentation. All chemicals and solvents were purchased from commercial sources and used as received without further purification. ESI-MS spectra were obtained on an Esquire 3000 Plus Bruker ion trap mass spectrometer. UV-Vis spectra were acquired on a UV 2550 Shimadzu spectrometer.

NMR spectra were acquired on 500 MHz (9.4 T) or 600 MHz (14.1 T) Bruker spectrometers. ^{19}F NMR spectra regarding responsive properties were acquired at 14.1 T (AQ = 0.03 s, TD = 0.03s, NS = 800, total time = 1 min). Relaxivity measurements and T_1-weighted MRI were performed on a 0.5 T NMR120-Analyst NMT Analyzing & Imaging system (Niumag Corporation). ^{19}F MRI were conducted on a Bruker 9.4 T BioSpec MRI system using an FLASH pulse sequence with the following parameters unless otherwise mentioned: FOV = 4.0 cm × 4.0 cm, MTX 32, SI = 11.00 mm, TR = 30.0 ms, TE = 1.3 ms, FA = 90.0 deg, TA = 10 min, NEX = 640. EPR spectra were acquired on an EMX-10/12 Bruker spectrometer.

Purification of the complexes was performed on a Shimadzu HPLC system (column: XBridge Prep C18 5 μm OBD 19 × 250 mm; total flow rate: 10 mL/min). An Agilent HPLC system (column: ZORBAX SB-C18 5 μm 9.4 × 250 mm; total flow rate: 1 mL/min) was used to trace the reduction of Mn(III)-HTFBED. 50 mM NH_4Ac buffer (pH = 7.4) and CH_3CN were used as eluents. Eluting conditions: 0–20 min, CH_3CN from 35% to 40%.

Cyclic voltammetry was performed on a CHI631 A Electrochemical Analyzer. Glassy carbon, Pt wire, and Ag/AgCl was used as the working electrode, the auxiliary electrode and the reference electrode, respectively.

Synthesis.

Synthesis of L1 from ethylenediamine is simple and straightforward (Scheme S1). Reaction of L1 with $MnCl_2 \bullet 4H_2O$ afforded Mn(II)-L1 smoothly, which was then subjected to facile aerobic oxidation to furnish Mn(III)-L1. Synthetic protocols and characterization of both complexes and intermediates are detailed below.

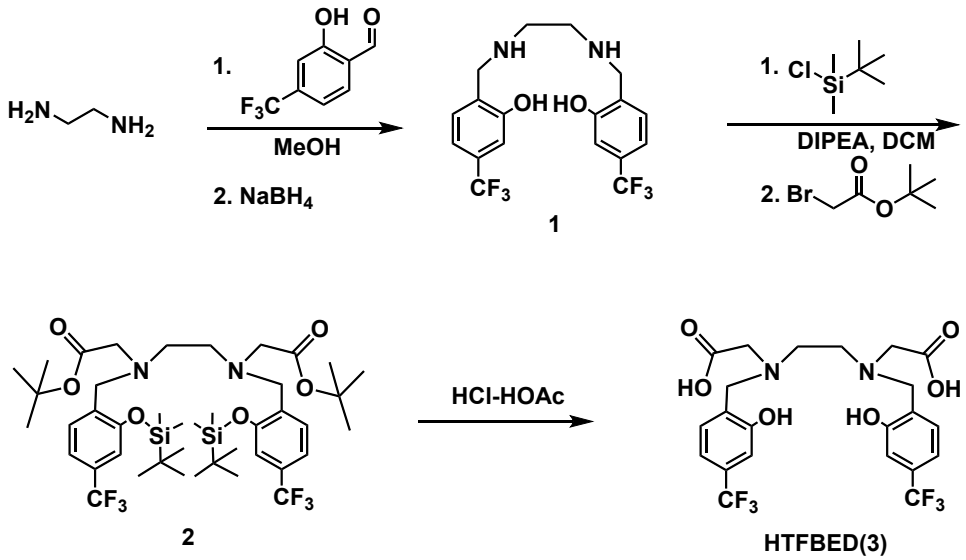

Scheme S1. Synthesis of *N,N′*-bis(2-hydroxy-4-trifluoromethylbenzyl)ethylenediamine-*N,N′*-diacetic acid (HTFBED, L1, **3**).

***N,N′*-Bis(2-hydroxy-4-trifluoromethylbenzyl)ethylenediamine (1)**

2-Hydroxy-4-(trifluoromethyl)benzaldehyde (1.0 g, 5.3 mmol) was dissolved in 200 mL methanol which was deoxygenated by bubbling N_2. A solution of 150 μL ethylenediamine (2.2 mmol) and 1.5 mL methanol was added. The resulting solution changed to bright yellow immediately. After 1 h stirring under N_2, $NaBH_4$ solid (0.7 g, 18.5 mmol) was added to the solution in five portions and the resulting solution turned colorless quickly. After 3 h stirring, the solvent was removed by a rotovap. 20 mL water and 100 mL dichloromethane was added to the white residue. The separated aqueous phase was extracted with dichloromethane (3 × 50 mL). All organic phases were combined, dried and concentrated to yield **1** (0.76 g, 83%) as a white solid: ^{1}H NMR (500 MHz, CD_3OD) δ 7.28 (d, J = 10 Hz, 2 H, Ar-H), 7.03 (d, J = 10 Hz, 2 H, Ar-H), 7.00 (s, 2 H, Ar-H), 3.96 (s, 4 H, Ar-CH_2N), 2.88 (s, 4 H, NCH_2CH_2N); ^{19}F NMR (470 MHz, CD_3OD) δ –64.18 (s); ESI-MS (m/z) calculated for $C_{18}H_{19}F_6O_2N_2$ $(M+H)^+$: 409.1, found: 408.8.

Di-*tert*-Butyl *N,N′*-bis(2-*tert*-butyldimethylsiloxy-4-trifluoromethylbenzyl)ethyl-enediamine-*N,N′*-diacetate (2)

1 (0.76 g, 1.9 mmol) was dissolved in 30 mL CH_2Cl_2 which was deoxygenated by bubbling N_2. Then the solution was cooled to −10 ºC and 1.65 mL *N*,*N*-diisopropylethylamine (DIPEA) was added. *tert*-Butyldimethylchlorosilane (633 mg, 4.2 mmol) in 3 mL CH_2Cl_2 was added over 20 min. The resulting solution was warmed to room temperature (RT) and stirred for 5 h. After that, the reaction was cooled to −30 ºC before a solution of *tert*-butyl bromoacetate (726 µL, 4.5 mmol) in 3 mL CH_2Cl_2 was added dropwise over 20 min. The resulting solution was warmed to RT and stirred for another 16 h. The solvent was removed by a rotovap. The residue was dissolved in 100 mL CH_2Cl_2, which was washed with water (3 × 100 mL). The organic phase was dried with anhydrous Na_2SO_4 and concentrated. The crude product was purified by flash chromatography on silica gel (EA/hexane = 1/200) to yield **2** (0.70 g, 57%) as a white solid: ^{1}H NMR (500 MHz, $CDCl_3$) δ 7.59 (d, *J* = 7.5 Hz, 2 H, Ar-H), 7.14 (d, *J* = 8.0 Hz, 2 H, Ar-H), 6.95 (s, 2 H, Ar-H), 3.77 (s, 4 H, Ar-CH_2N), 3.27 (s, 4 H, $COCH_2$), 2.78 (s, 4 H, NCH_2CH_2N), 1.42 (s, 18 H, $OC(CH_3)_3$), 0.99 (s, 18 H, $SiC(CH_3)_3$), 0.21 (s, 12H, $Si(CH_3)_2$); ^{19}F NMR (470 MHz, CD_3OD) δ −62.46 (s); ESI-MS (m/z) calculated for $C_{42}H_{67}F_6O_6N_2Si_2$ $(M+H)^+$: 865.4, found: 865.4.

_N,N′_-bis(2-hydroxy-4-trifluoromethylbenzyl)ethylenediamine-_N,N′_-diacetic acid (3, HTFBED, L1)

2 (0.70 g, 0.8 mmol) was dissolved in 30 mL acetic acid before 15 mL 37% hydrochloric acid was added. The resulting solution was stirred at 40 ºC for 10 h with liquid sealing, then the solvent was removed by a rotovap. The residue was dissolved with 37% hydrochloric acid (3 × 10 mL) and solvent was removed by a rotovap to yield **3**•2HCl (0.38 g, 79%) as a white solid: ^{1}H NMR (500 MHz, CD_3OD) δ 7.52 (d, *J* = 10 Hz, 2 H, Ar-H), 7.20 (d, *J* = 5.0 Hz, 2 H, Ar-H), 7.16 (s, 2 H, Ar-H), 4.36 (s, 4 H, Ar-CH_2N), 3.86 (s, 4 H, COCH2), 3.52(s, 4 H, NCH_2CH_2N); ^{13}C NMR (127 MHz, CD_3OD) δ 172.12 (2 C), 157.97 (2 C), 134.08 (2 C), 134.02-133.26 (m, 2 C), 124.07-128.39 (m, 2 C), 124.41 (2 C), 117.57 (2 C), 113.40 (2 C), 54.58 (2 C), 54.26 (2 C), 51.69 (2 C); ^{19}F NMR (470 MHz, CD_3OD) δ (ppm): −64.55 (s); HR-ESI-MS (m/z) calculated for $C_{22}H_{23}F_6O_6N_2$ $(M+H)^+$: 525.1460, found: 525.1496.

Mn(II)-HTFBED (Mn(II)-L1)

150 mg **3**•2HCl (0.25 mmol) was dissolved in 50 mL water with pH at 8.0 under N_2. 49 mg $MnCl_2.4H_2O$ (0.25 mmol) was added. The pH of the resulting suspension was adjusted to 8.0 carefully with 0.1 M NaOH solution. The resulting clear solution was stirred for 1 h before ascorbic acid (ca. 10.0 mg) was added and the pH of the solution was adjusted to 7.5. The mixture was purified by HPLC

and lyophilization to yield Mn(II)-L1 as a white solid: ^{19}F NMR (600 MHz, D_2O) δ −65.76 (bs); HR-ESI-MS (m/z) calculated for $MnC_{22}H_{19}F_6O_6N_2$ $(M+H)^-$: 576.0528, found: 576.0504.

Mn(III)-HTFBED (Mn(III)-L1)

150 mg HTFBED•2HCl (0.25 mmol) was dissolved in 50 mL water with pH at 8.0 under N_2. 49 mg $MnCl_2.4H_2O$ (0.25 mmol) was added. The pH of the resulting suspension was adjusted to 8.0 carefully with 0.1 M NaOH solution. The resulting clear solution was stirred for 10 h at 40 ºC under air, then the pH of the solution was adjusted to 7.5. The mixture was purified by HPLC and lyophilization to yield Mn(III)-L1 as a brown solid: ^{19}F NMR (576 MHz, D_2O) δ −75.89 (s); HR-ESI-MS (m/z) calculated for $MnC_{22}H_{18}F_6O_6N_2$ M^-: 575.0450, found: 575.0428.

Cell culture

Cells mentioned in the article were purchased from the Cell Bank of Type Culture Collection of Chinese Academy of Sciences. HepG2 cells were cultured according to ATCC recommended protocols. Briefly, all the cells were maintained in an atmosphere with 5% CO_2 at 37 °C and cultured in Dulbecco's Modified Eagle Medium (DMEM, Gibco) supplemented with 10% fetal bovine serum.

Cellular ^{19}F NMR

HepG2 cells (~2×10^6) were first incubated with 0.17 mM Mn(III)-L1 for 4 h. After washed and collected into a 1.5 mL centrifuge tube, cells were then treated for 20 min with 100 μM ascorbic acid (AA). Cells treated with Mn(III)-L1 only were used as a positive control. Before ^{19}F NMR analysis, cells were washed with 600 μL PBS for three times and finally suspended in 500 μL PBS. D_2O (100 uL) was added to the suspension. ^{19}F NMR spectra was acquired at 14.1 T with the following parameters: F19CPD-PABBFO sequence, AQ = 0.03 s, TD = 0.03 s, NS = 2000, total time =3 min.

HepG2 cells (~2×10^6) were first incubated with 0.17 mM Mn(II)-HTFBED for 4 h. After washed and collected into a 1.5 mL centrifuge tube, cells were then treated for 20 min with 50 nM pyocyanin (an endogenous ROS inducer), or 90 μM carbonyl cyanide *m*-chlorophenyl hydrazone (CCCP, an oxidative phosphorylation uncoupler). Cells treated with 5 mM *N*-acetylcysteine amide (NAC, a membrane-penetrating antioxidant) after stimulated with pyocyanin or Mn(II)-L1 only were used as negative controls. The rest of the experiment was the same as the above one.

Cellular ^{19}F MRI

HepG2 cells (~1×10^7) were first incubated with 50 nM pyocyanin for 1 h. Then the cells were trypsinized and incubated with 1 mM Mn(II)-L1 for 1 h. Cells directly treated with 1 mM Mn(II)-L1 or Mn(III)-L1 were used as a negative or positive control, respectively. After washed with PBS for three times, cells were suspended in 150 μL PBS and transferred to 500 μL centrifuge tubes. ^{19}F MRI was acquired at 9.4 T with the following parameters: FLASH sequence, FOV = 4.5 cm × 4.5 cm, SI = 8 mm, TR = 30.0 ms, TE = 1.3 ms, FA = 90.0 deg, NEX = 1800, TA = 29 min.

Table S1. ^{19}F relaxation times of L1 ligand, Mn(II)-L1, and Mn(III)-L1, measured at 9.4 T or 14.1 T.

	T_1 (ms)		T_2 (ms)		T_2/T_1	
Magnetic field strength	9.4 T	14.1 T	9.4 T	14.1 T	9.4 T	14.1 T
L1	955	772	629	471	0.66	0.61
Mn(II)-L1	1.6	1.7	0.6	0.6	0.38	0.35
Mn(III)-L1	6.4	5.4	4.0	2.7	0.63	0.50

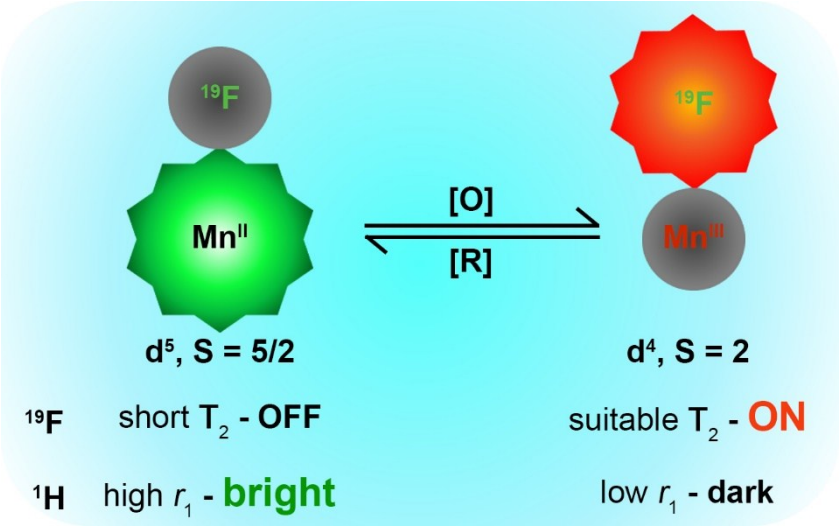

Figure S1. Schematic illustration of a pair of reversible redox-responsive manganese(II)/(III) complexes for contrast-enhanced ^{1}H MRI and ^{19}F MRI. ^{19}F signals of Mn(II) complex are "quenched" by paramagnetic Mn(II) as the T_2 of ^{19}F nuclei is significantly shortened while Mn(III) complex has strong ^{19}F signals due to the suitable T_2 of ^{19}F nuclei. Mn(II) complex with more single electrons has higher r_1 than Mn(III) complex, resulting in better contrast enhancement for ^{1}H MRI.

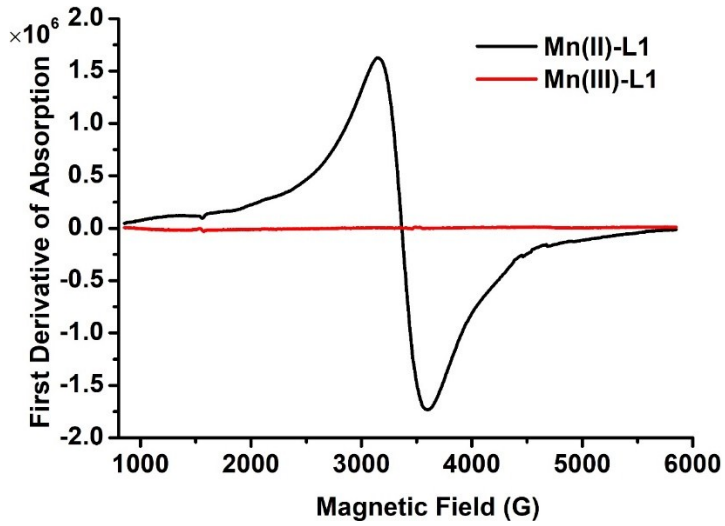

Figure S2. EPR characterization of Mn (II)-L1 and Mn (III)-L1 at 100 K. 8 mM Mn(II)-L1 and 8 mM Mn(III)-L1 aqueous solutions were frozen with liquid nitrogen respectively before measurement.

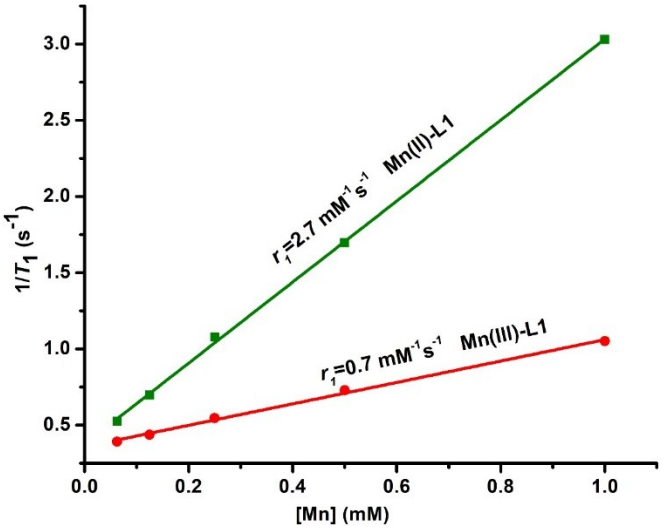

Figure S3. Longitudinal relaxivities (r_1) of Mn (III)-L1 (red line) and Mn (II)-L1 (green line) measured on a 0.5 T Niumag NMI20-Analyst system (Suzhou Niumag Analytical Instrument Corporation).

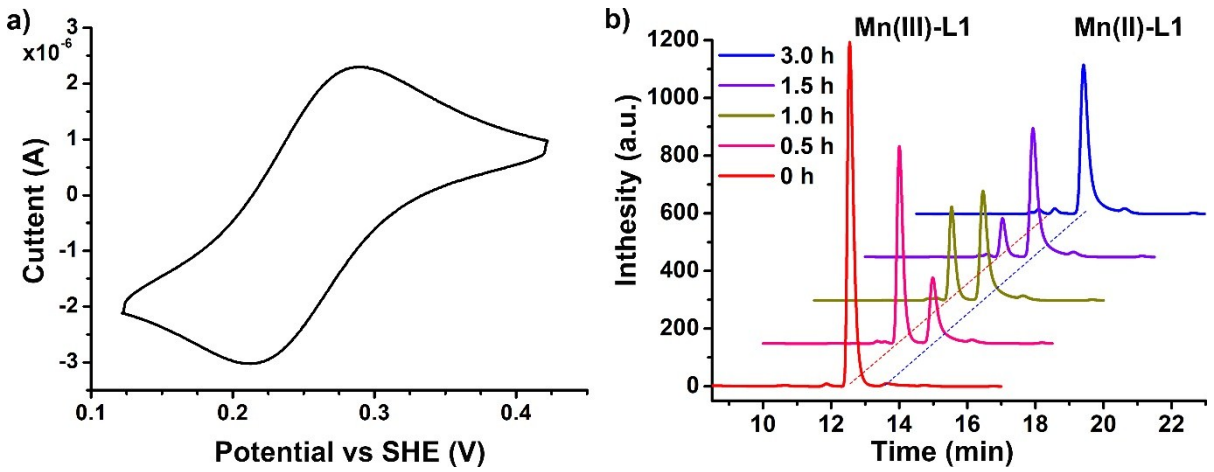

Figure S4. (a) Cyclic voltammogram of 0.5 mM Mn(III)-L1 in pH 7.4 HEPES buffer with a scan rate at 10 mV/s, showing a redox potential at 0.25 V *vs* SHE. (b) HPLC traces of the products of Mn(III)-L1 reduced by DTT at different time points. HPLC traces reveal a smooth reduction process with the content of Mn(III)-L1 decreasing and that of Mn(II)-L1 increasing over time.

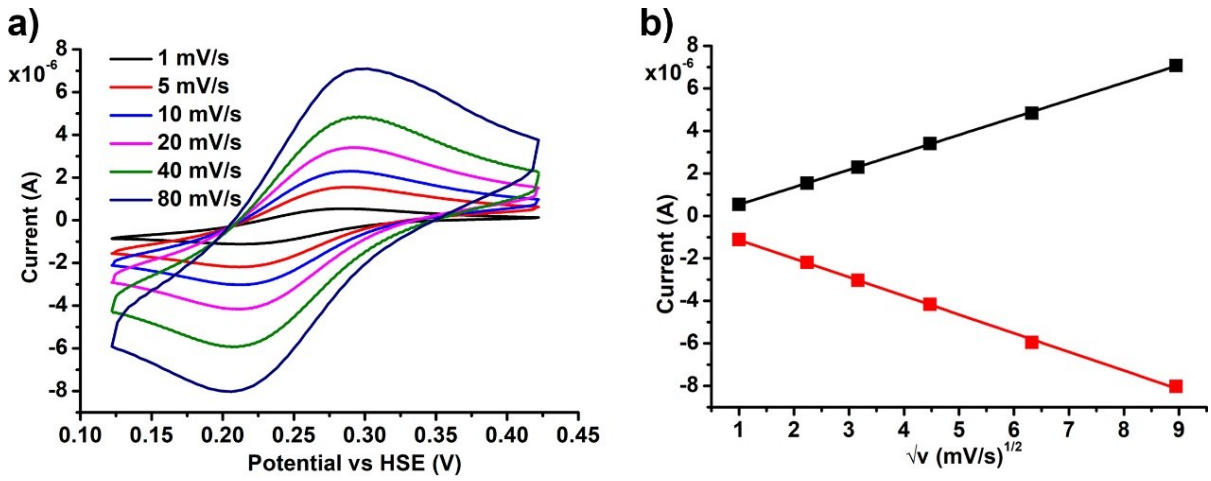

Figure S5. (a) Cyclic voltammogram of 0.5 mM Mn (III)-HTFBED in HEPES buffer (100 mM, pH = 7.4, containing 0.1 M KCl as the supporting electrolyte) with different scan rates. (b) Corresponding linear fitting for peak currents *versus* the square root of scan rates.

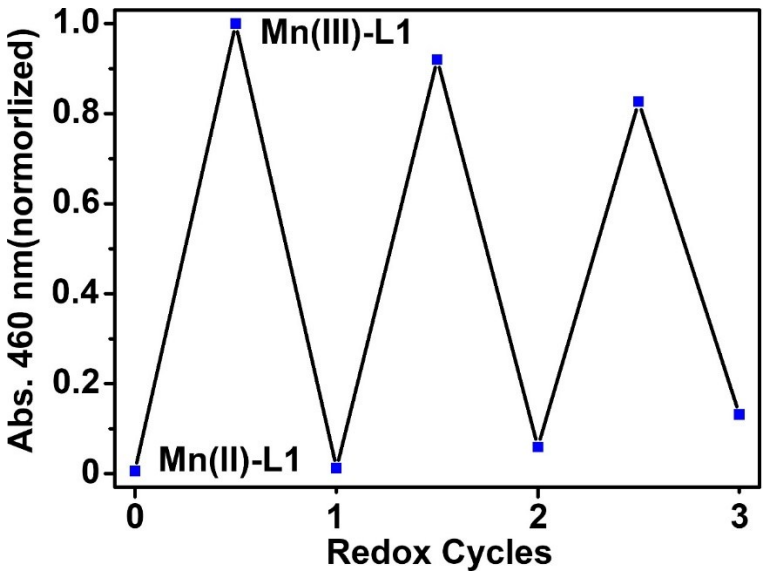

Figure S6. UV-Vis absorption (absorbance at 460 nm) analysis of Mn(II)-L1 (1 mM in 100 mM pH 7.4 HEPES) response to air/AA redox cycles, which reveals the sensitive response of Mn(II)-L1 to air/ascorbic acid (AA) redox cycles and indicates that the probes are stable after three redox cycles.

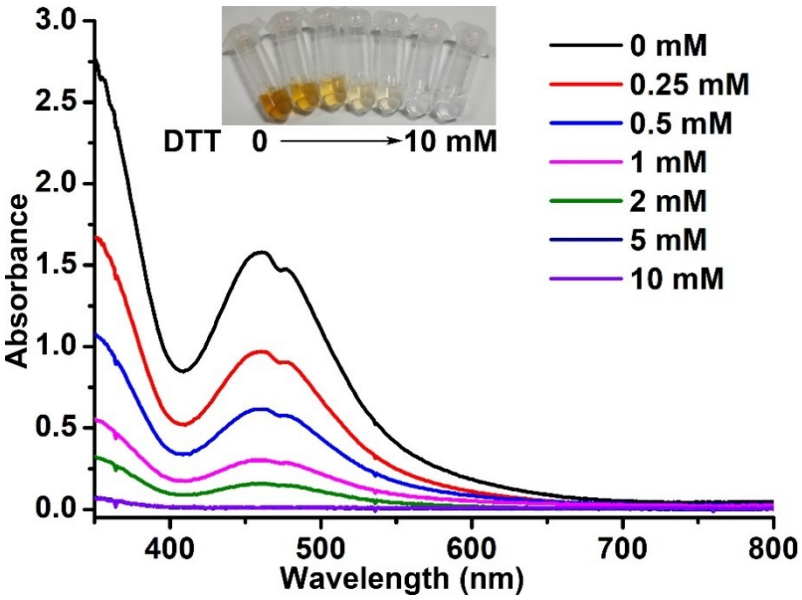

Figure S7. UV-Vis absorption spectra of 1 mM Mn(III)-L1 after incubated with different concentrations of DTT in HEPES buffer (100 mM, pH = 7.4) for 3 h. Inset is the corresponding optical photographs with DTT concentration increasing from left to right. With the elevation of DTT concentration, the color of the solution changes from brown (Mn(III)-L1) to colorless (Mn(II)-L1) and the characteristic UV-Vis absorption of Mn(III)-L1 disappears, suggesting the conversion of Mn(III)-L1 to Mn(II)-L1.

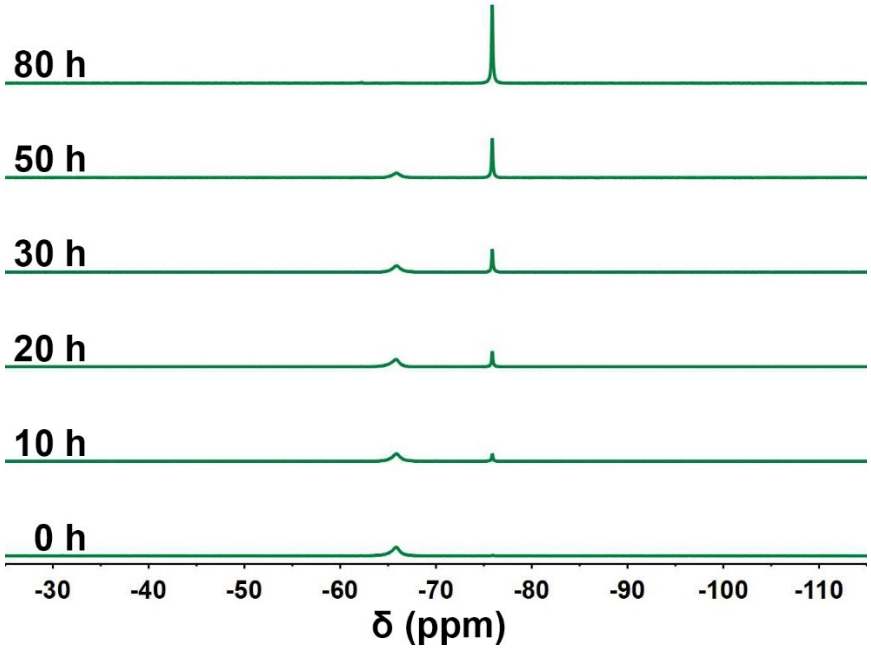

Figure S8. Characterization of air oxidation of Mn(II)-L1 (1 mM) in HEPES buffer (100 mM, pH = 7.4, 37 ºC) by ^{19}F NMR.

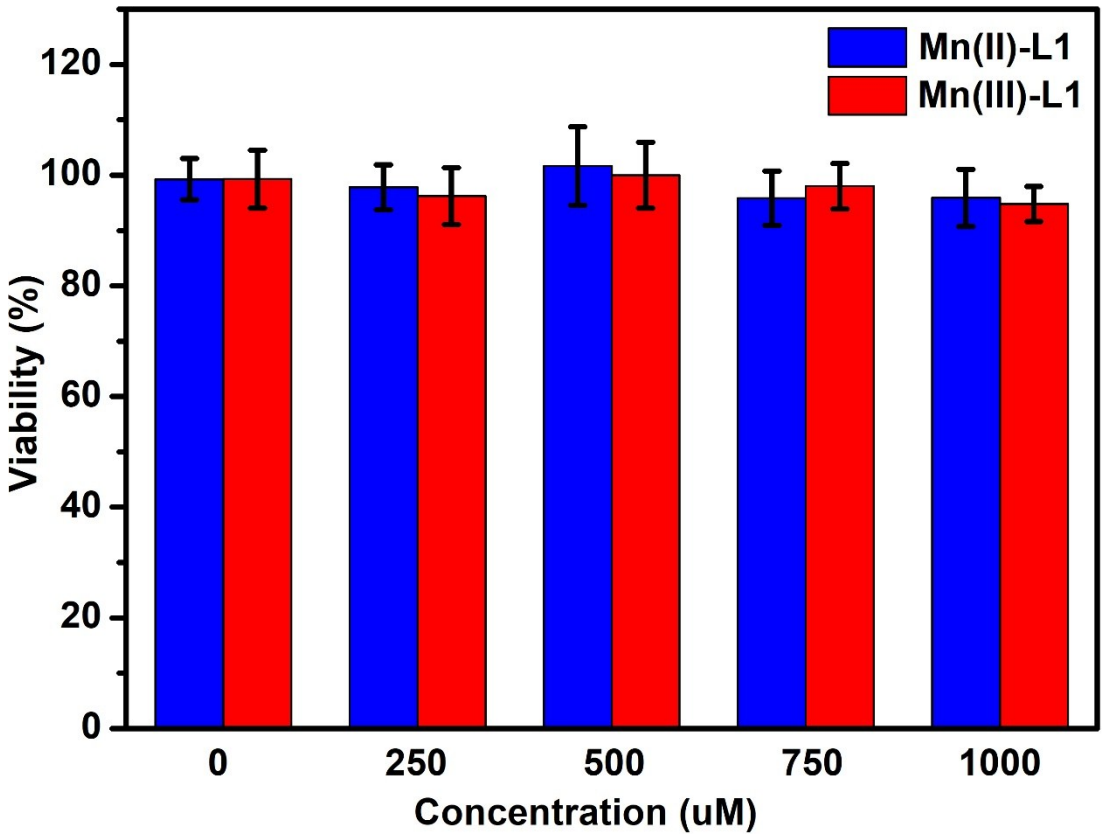

Figure S9. Cytotoxicity of Mn(II)/(III)-L1 against HepG2 cells evaluated *via* MTT assays.

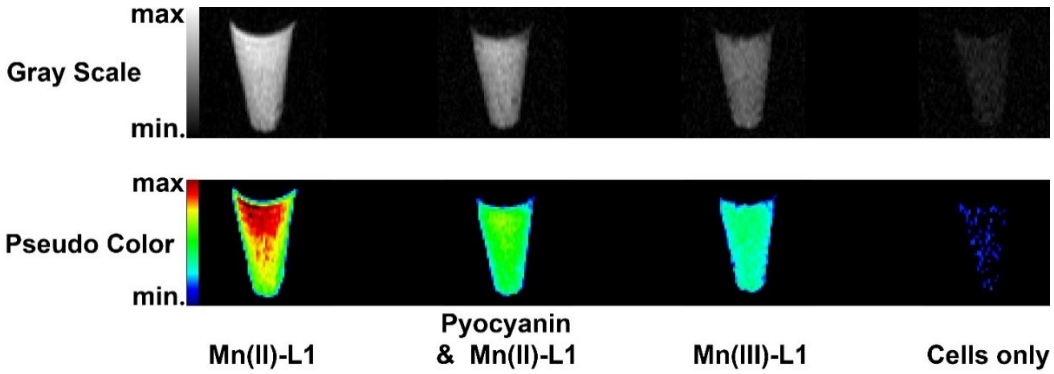

Figure S10. ^{1}H MRI grey scale and pseudo color images of HepG2 cells subjected to treatments as indicated.

^{1}H NMR, ^{19}F NMR and ESI-MS spectra of **1**

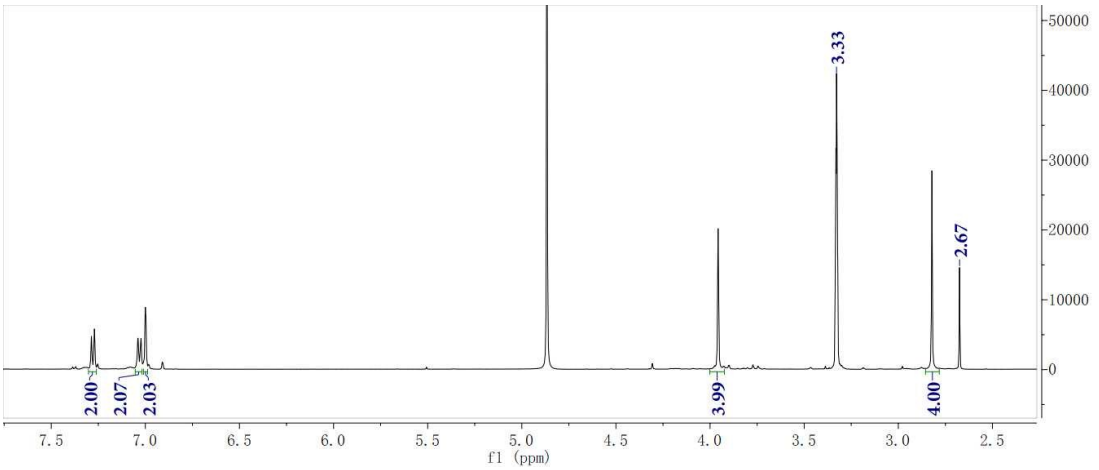

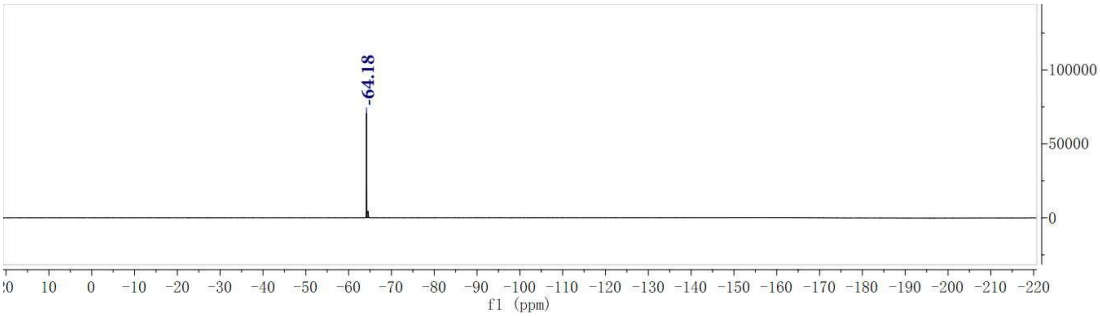

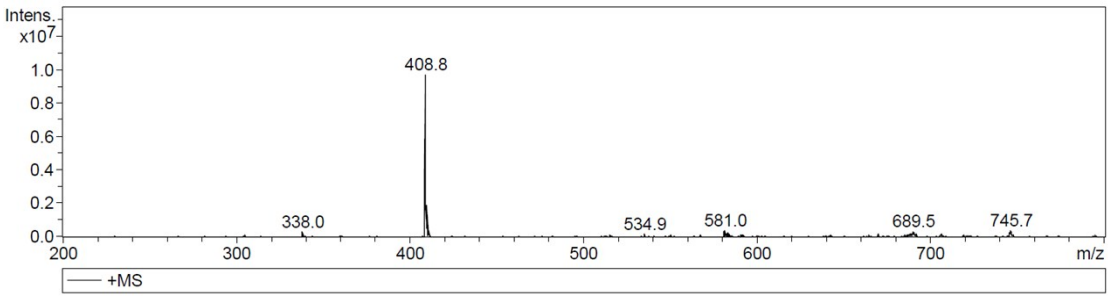

^{1}H NMR, ^{19}F NMR and ESI-MS spectra of **2**

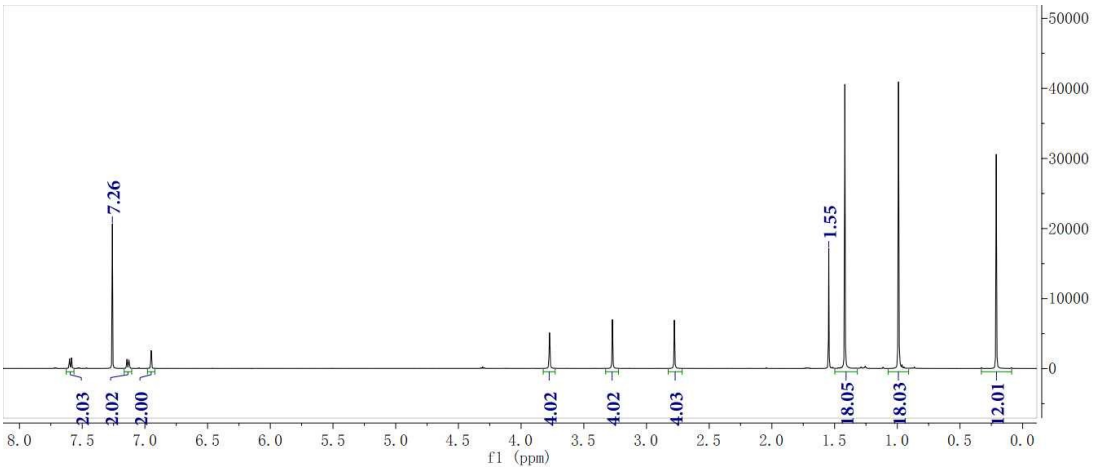

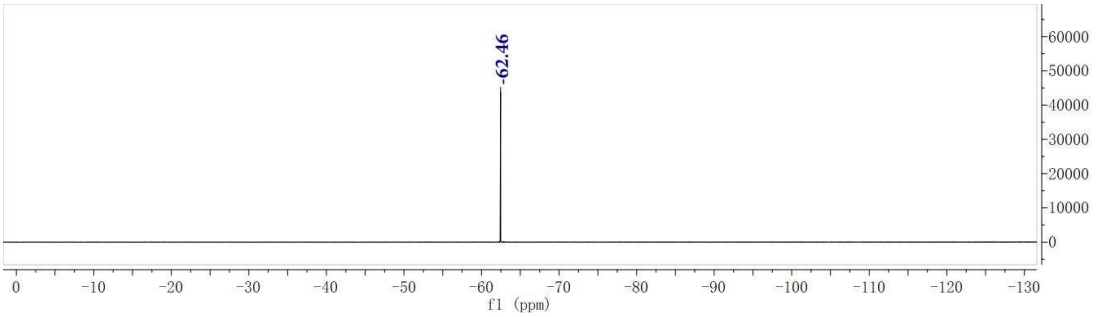

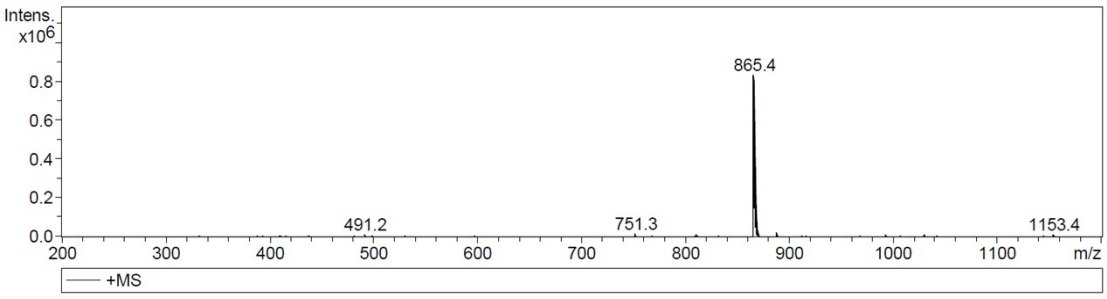

^{1}H NMR, ^{19}F NMR, and ^{13}C NMR spectra of **3** (L1)

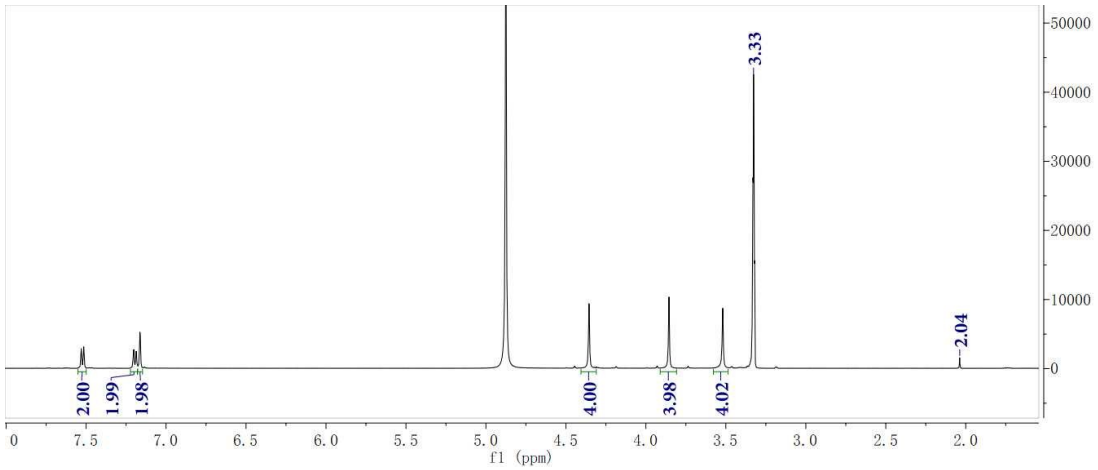

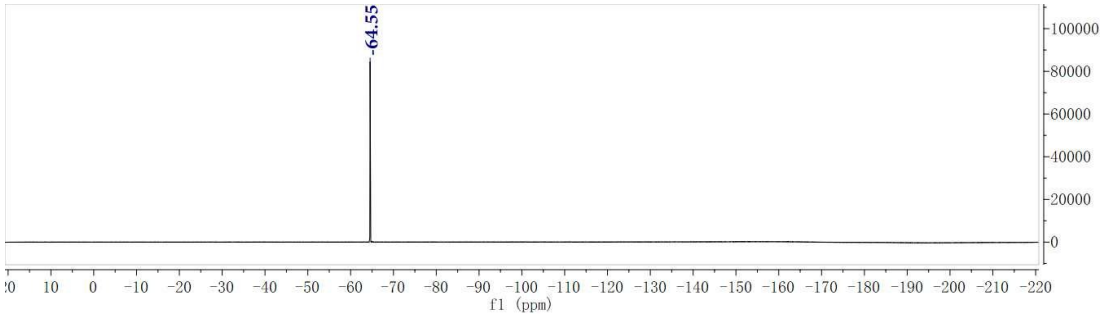

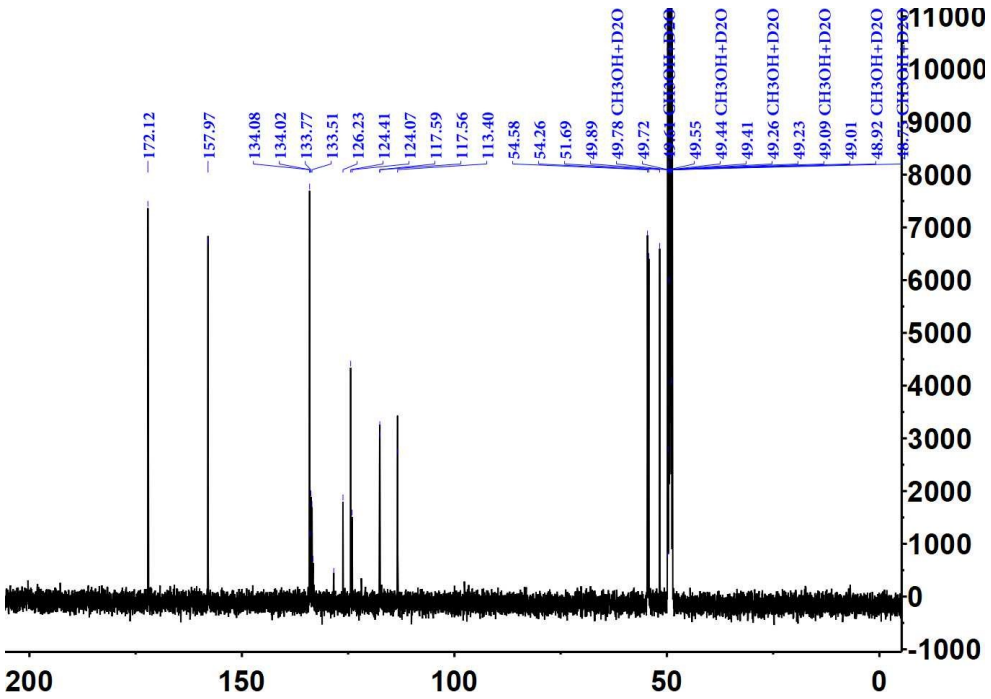

HR-ESI-MS spectrum of **3** (L1)

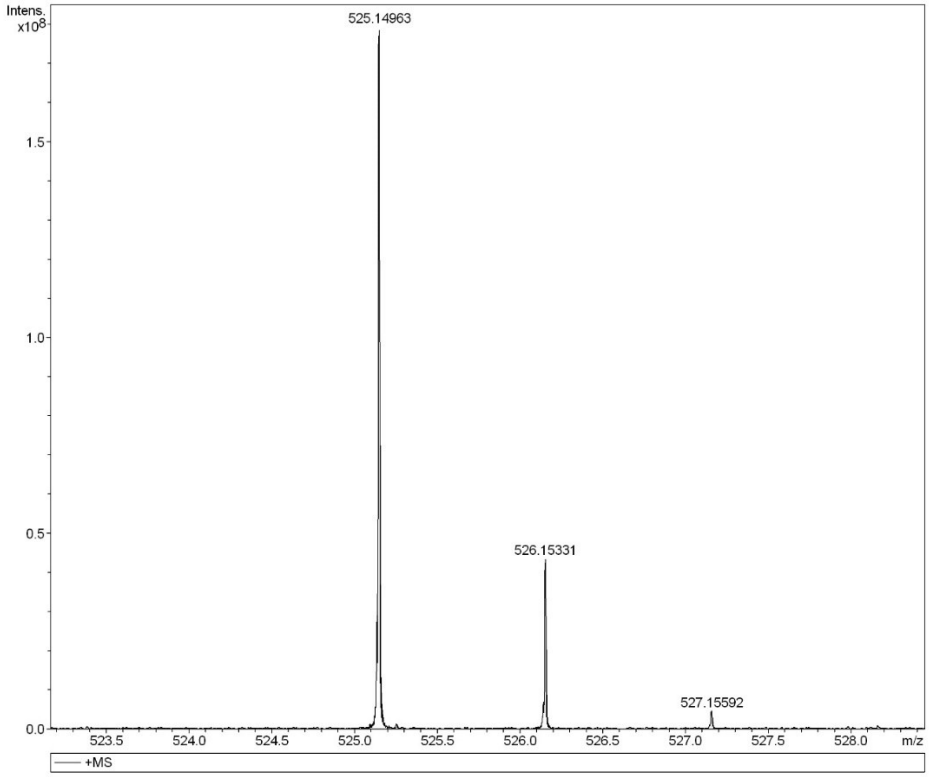

^{19}F NMR and HR-ESI-MS spectra of Mn(II)-L1.

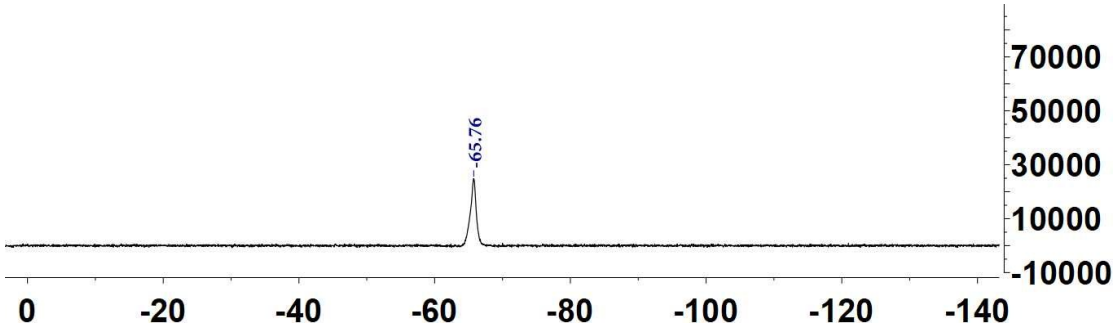

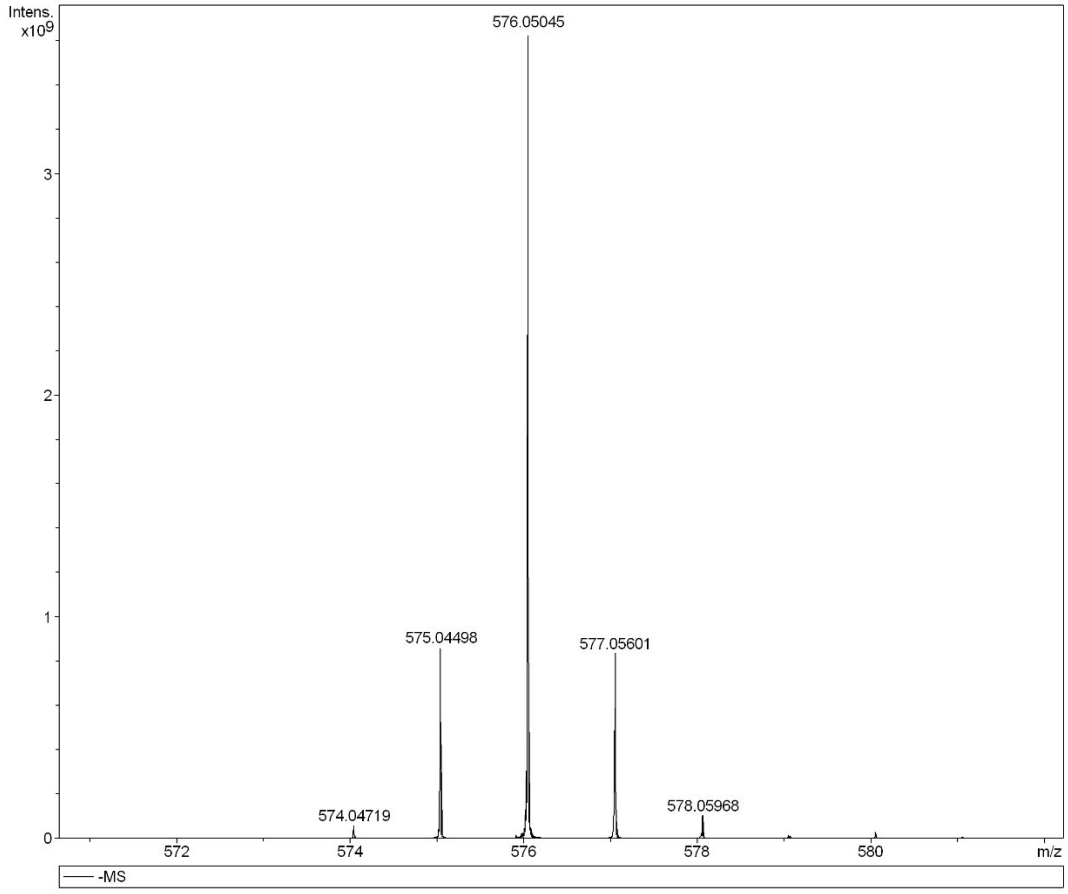

^{19}F NMR and HR-ESI-MS spectra of Mn(III)-L1.